

Real-time assessment of *Candida* biofilm formation

Pedro MDS Abrantes, Kauthar Behardien, Charlene WJ Africa

Maternal Endogenous Infections Studies (MENIS) Research Laboratories, Department of Medical Biosciences,
University of the Western Cape, Bellville, South Africa



UNIVERSITY of the
WESTERN CAPE

60 YEARS
of hope, action
& knowledge



- *Candida* species are known to form highly structured biofilms surrounded by extracellular polymeric substances (EPS), providing microbial communities with metabolic cooperation and protection from the external environment and antimicrobial drugs¹.
- Drug-resistant, non-*albicans* species have emerged and are on the increase due to severe patient immunosuppression or the indiscriminate use of broad-spectrum antimicrobials, leading to increased patient morbidity and mortality².
- We have previously reported differences in the distribution and antimicrobial profiles of HIV-associated *Candida* in two African regions³, with *C. albicans*, *C. dubliniensis* and *C. glabrata* being present in both populations and *C. tropicalis*, *C. krusei* and *C. parapsilosis* only found in one region.
- The real-time biofilm formation of *Candida* species consortia has not been previously described, which would establish whether specific species may enhance or inhibit the rate of biofilm formation.

- The type strains used in this study included *Candida albicans* (ATCC 90028), *Candida dubliniensis* (NCPF 3949a), *Candida glabrata* (ATCC 26512), *Candida tropicalis* (ATCC 950), *Candida krusei* (ATCC 2159) and *Candida parapsilosis* (ATCC 22019). Individual *Candida* species were tested, as well as combinations of common and less commonly isolated species.
- The real-time biofilm formation was assessed using an xCELLigence real time cell analyser (RTCA), by growing the organisms in YPD broth on 16-well E-plates with embedded gold microelectrodes and measuring the cell adhesion / extracellular polymeric substances (EPS) formation with impedance readings set to take place at 15-minute intervals. The real-time cell index (CI) values for the full duration of the experiments were then plotted in individual graphs.

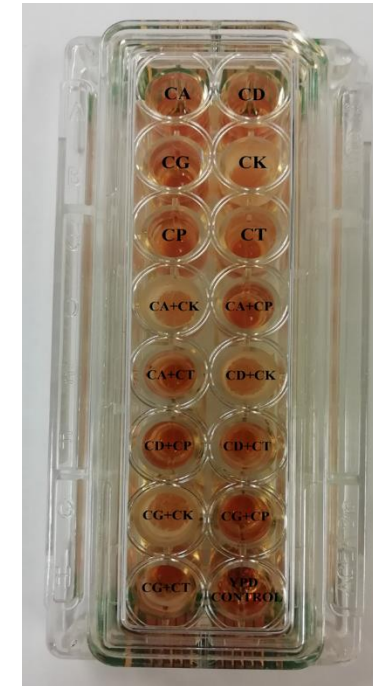


Figure 1. Experimental procedure of individual (100 μ l) and mixed (50 μ l + 50 μ l) *Candida* suspensions on a gold microelectrode-embedded E-plate 16. CA: *Candida albicans*; CD: *Candida dubliniensis*; CG: *Candida glabrata*; CK: *Candida krusei*; CP: *Candida parapsilosis*; CT: *Candida tropicalis*.

- Bulk biofilm morphology was observed by growing the organisms in RPMI-1640 medium on 12-well cell culture plates for 24 h and 48 h, followed by staining with calcofluor white stain and 10% KOH solution and observing at 40X under UV light using an epi-fluorescence inverted microscope.
- Crystal violet (CV) staining was carried out by growing the organisms in RPMI-1640 medium on 96-well microtiter plates for 66 h and staining with 0.4% aqueous CV solution, followed by de-staining in 95% ethanol and measuring the absorbance at OD₅₉₅ using a plate reader.



Figure 2. Forty-eight hour bulk biofilm formation seen at the bottom of 12-well cell culture plates, after cells were washed and before CFW/KOH staining and FM observation.

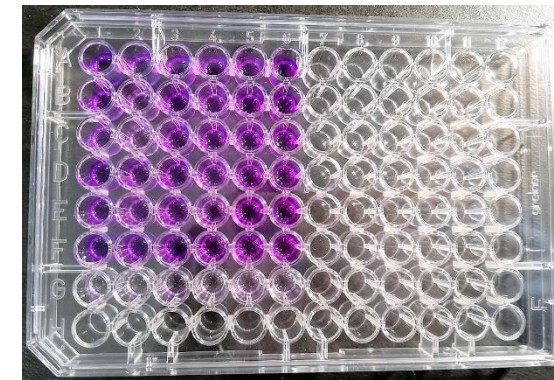


Figure 3. Crystal violet staining assay.

Real-time biofilm formation

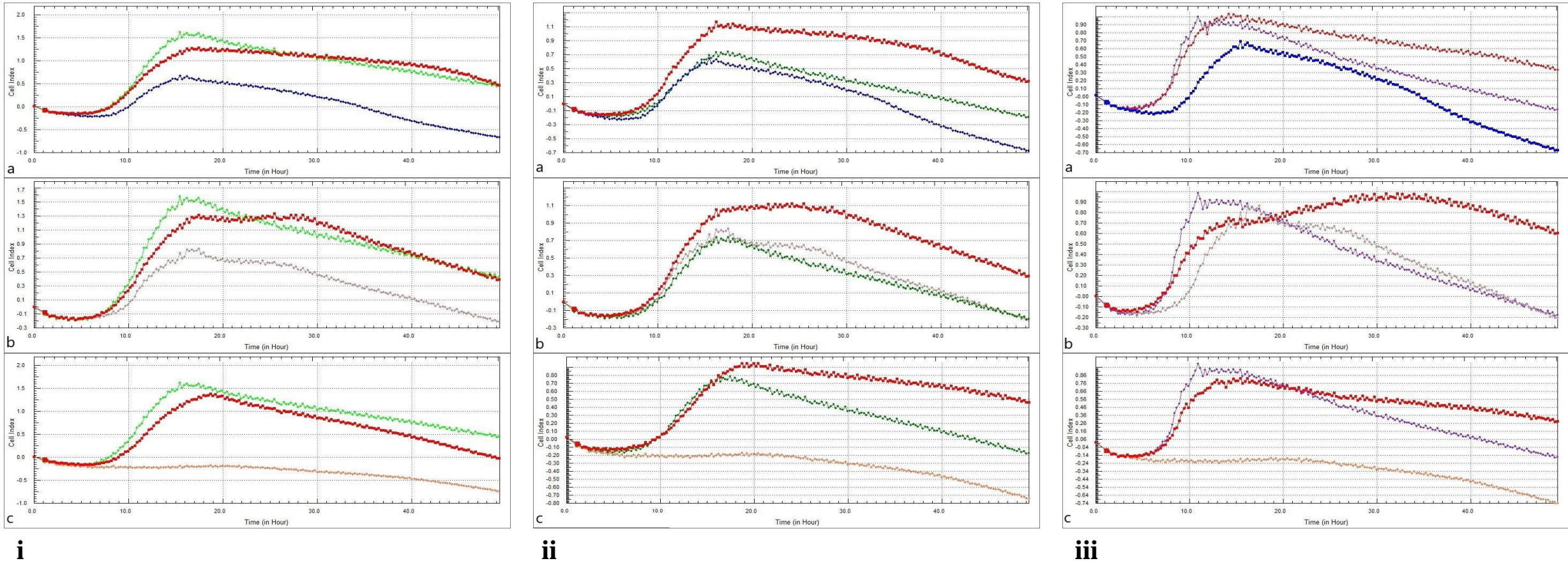


Figure 4. Cell index variations of **(i)** *C. albicans* (light green), **(ii)** *C. dubliniensis* (dark green) and **(iii)** *C. glabrata* (purple) with **(a)** *C. tropicalis* (blue), **(b)** *C. krusei* (light grey) and **(c)** *C. parapsilosis* (coral) biofilm formation, with the mixed adhesion shown in red.

Monospecies bulk biofilm morphology

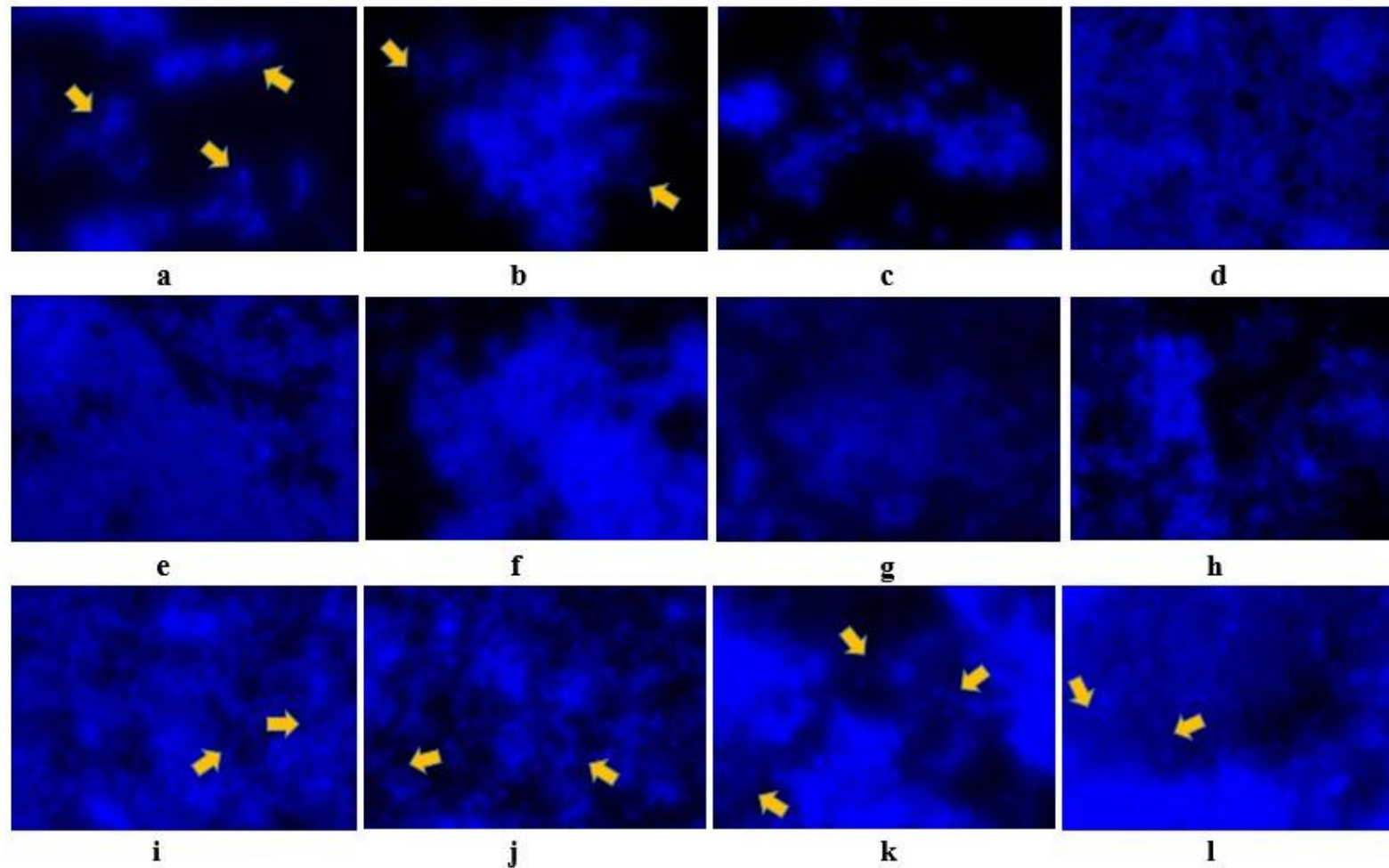


Figure 5. Fluorescence microscopy of early (24 h) and mature (48 h) biofilms of *C. albicans* (a and b), *C. dubliniensis* (c and d), *C. glabrata* (e and f), *C. krusei* (g and h), *C. parapsilosis* (i and j) and *C. tropicalis* (k and l). An increase in biofilm mass is shown as confluent growth in the well surface and increased fluorescence, and was most noticeable in *C. albicans*, *C. dubliniensis*, *C. glabrata* and *C. tropicalis*. *Candida parapsilosis* failed to demonstrate a noticeable increase in biofilm mass between 24 and 48 h when grown on its own. Filamentous structures were observed in *C. albicans*, *C. parapsilosis* and *C. tropicalis* biofilms (orange arrows). A transparent mass surrounding large clusters of cells was also observed, an indication of EPS formation.

Mixed species bulk biofilm morphology

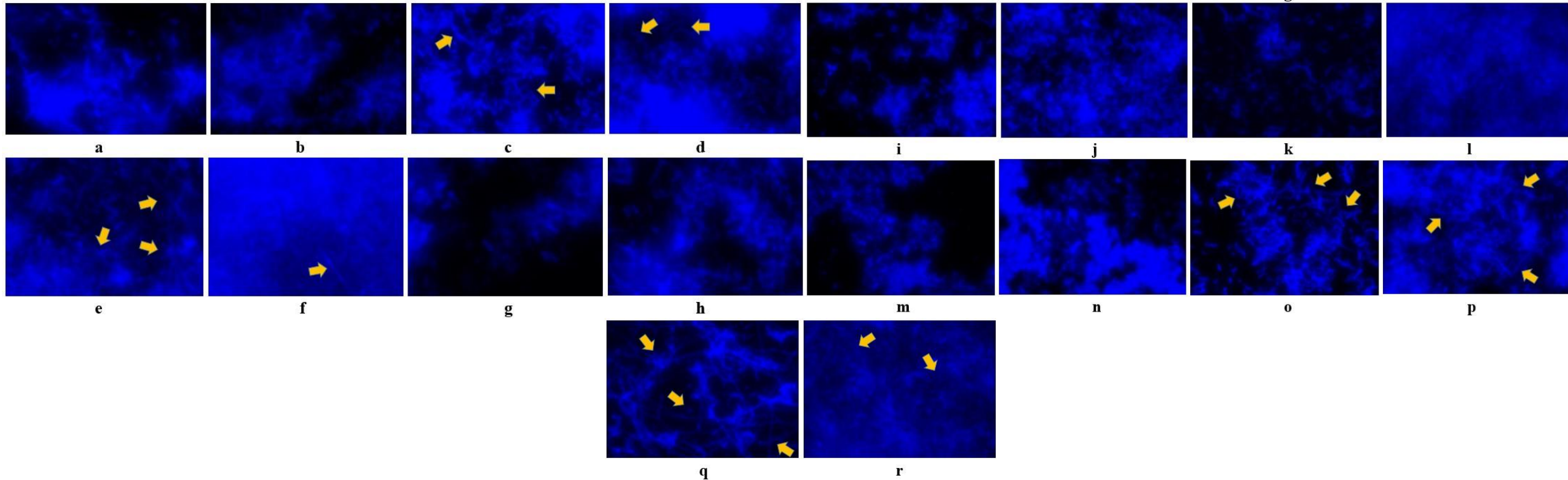
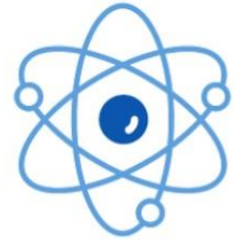


Figure 6. Fluorescence microscopy of early (24 h) and mature (48 h) mixed biofilms of *C. albicans*/*C. krusei* (**a** and **b**); *C. albicans*/*C. parapsilosis* (**c** and **d**); *C. albicans*/*C. tropicalis* (**e** and **f**); *C. dubliniensis*/*C. krusei* (**g** and **h**); *C. dubliniensis*/*C. parapsilosis* (**i** and **j**); *C. dubliniensis*/*C. tropicalis* (**k** and **l**); *C. glabrata*/*C. krusei* (**m** and **n**); *C. glabrata*/*C. parapsilosis* (**o** and **p**); *C. glabrata*/*C. tropicalis* (**q** and **r**). Increased cell density was most noticeable in the interactions of *C. albicans* with *C. tropicalis* and *C. parapsilosis*, *C. dubliniensis* interactions with *C. parapsilosis* and *C. tropicalis* and *C. glabrata* interactions with *C. parapsilosis* and *C. tropicalis*. Extensive filamentous structures were present when *C. albicans* and *C. glabrata* were grown in combination with either *C. tropicalis* or *C. parapsilosis* (orange arrows).

Bulk biofilm quantification

- When looking at the bulk biofilm production of individual species, *C. albicans* formed the greatest amount of biofilm, followed by *C. tropicalis* and the other species (*C. albicans* > *C. tropicalis* > *C. krusei* > *C. parapsilosis* > *C. dubliniensis* > *C. glabrata*).
- The biofilm production of combined species was the highest for *C. albicans/C. tropicalis* followed by the mixed biofilm combinations of these and other species (*Ca/Ct* > *Cg/Ct* > *Cd/Ct* > *Ca/Cp* > *Ca/Ck* > *Cg/Ck* > *Cd/Ck* > *Cd/Cp* > *Cg/Cp*).

- When using both the conventional CV staining method and the novel xCELLigence system, *C. albicans* demonstrated the highest absorbance/impedance values when compared to the other species studied, supporting previous studies which have described it as the most notorious biofilm former of all pathogenic yeasts^{1,4}.
- Most xCELLigence mixed growth curves appeared to follow similar (albeit increased) adhesion, maturation and detachment phase curves, an interpretation of biofilm formation first described by Gutiérrez *et al*⁵. The xCELLigence system also showed that the combined growth of *C. glabrata* and *C. krusei* resulted in increased adhesion (increase in CI values) and biofilm maturation (peak CI value) over 30 h, with the detachment phase (declining slope after peak CI value) also starting much later.
- The extensive filamentation seen in *C. albicans* biofilm formations with *C. tropicalis* and *C. parapsilosis*^{6,7} and the increasingly azole-resistant *C. glabrata*⁸ is worthy of note, since the switch to pseudohyphal and hyphal morphologies has been associated with increased invasion, penetration and growth in between host epithelial cells⁹, endothelial cell damage¹⁰ and destruction of immune cells following phagocytosis¹¹.
- Although *C. parapsilosis* did not form biofilms when grown on its own using the xCELLigence system, it resulted in increased CI values over time when combined with *C. dubliniensis* and *C. glabrata*. These results could be explained by the fact that the xCELLigence system takes into consideration various factors such as the adhesion and EPS formation (as opposed to only the bulk biofilm formation measured by CV staining). This system also monitors changes in cell number and size and provides continuous and automated data analysis, thereby having an advantage over traditional biofilm staining and quantification assays¹².
- The results of this study suggest that the biofilm formation of *C. tropicalis*, *C. krusei* and *C. parapsilosis* is influenced by the presence of *C. albicans*, *C. dubliniensis* and *C. glabrata*, all of which have different antifungal susceptibility profiles. This is important for the consideration and application of antifungal drugs for the treatment of resistant *Candida* biofilms.



FACULTY *of*
NATURAL SCIENCES
UNIVERSITY *of the* WESTERN CAPE



The authors gratefully acknowledge ACEA Biosciences (San Diego, CA) and Anatech Analytical Technology (Johannesburg, South Africa) for the use of the xCELLigence RTCA equipment, Christelle Klopper from Anatech Instruments for her excellent technical advice and Prof. David Fisher from the Neurobiology Research Group, Department of Medical Biosciences, UWC, for the use of the fluorescence microscope.

This study was partially supported financially by the National Research Foundation of South Africa.

1. Ramage, G., Mowat, E., Jones, B., Williams, C. & López-Ribot, J. L. Our current understanding of fungal biofilms. *Crit. Rev. Microbiol.* **35**, 340-355 (2009).
2. Pfaller, M. A. & Diekema, D. J. Epidemiology of invasive candidiasis: a persistent public health problem. *Clin. Microbiol. Rev.* **20**, 133-163 (2007).
3. Abrantes, P. M. D. S., McArthur, C. P. & Africa, C. W. J. Multi-drug resistant oral *Candida* species isolated from HIV-positive patients in South Africa and Cameroon. *Diagn. Microbiol. Infect. Dis.* **79**, 222-227 (2014).
4. Nobile, C. J. & Johnson, A. D. *Candida albicans* biofilms and human disease. *Annu. Rev. Microbiol.* **69**, 71-92 (2015).
5. Gutiérrez, D., Hidalgo-Cantabrana, C., Rodríguez, A., García, P. & Ruas-Madiedo, P. Monitoring in real time the formation and removal of biofilms from clinical related pathogens using an impedance-based technology. *PLoS One* **11**, e0163966 (2016).
6. Juyal, D., Sharma, M., Pal, S., Rathaur, V. K. & Sharma, N. Emergence of non-*albicans Candida* species in neonatal candidemia. *N. Am. J. Med. Sci.* **5**, 541-545 (2013).
7. Sadeghi, G., Ebrahimi-Rad, M., Mousavi, S. F., Shams-Ghahfarokhi, M. & Razzaghi-Abyaneh, M. Emergence of non-*Candida albicans* species: Epidemiology, phylogeny and fluconazole susceptibility profile. *J. Mycol. Med.* **28**, 51-58 (2018).
8. Whaley, S. G. & Rogers, P. D. Azole resistance in *Candida glabrata*. *Curr. Infect. Dis. Rep.* **18**, 41 (2016).
9. Kumamoto, C. A. & Vines, M. D. Contributions of hyphae and hypha-co-regulated genes to *Candida albicans* virulence. *Cell Microbiol.* **7**, 1546-1554 (2005).
10. Jong, A. Y., Stins, M. F., Huang, S. H., Chen, S. H. & Kim, K. S. Traversal of *Candida albicans* across human blood-brain barrier *in vitro*. *Infect. Immun.* **69**, 4536-4544 (2001).
11. Korting, H. C. *et al.* Reduced expression of the hyphal-independent *Candida albicans* proteinase genes SAP1 and SAP3 in the *efg1* mutant is associated with attenuated virulence during infection of oral epithelium. *J. Med. Microbiol.* **52**, 623-632 (2003).
12. van Duuren, J. B. J. H. *et al.* Use of single-frequency impedance spectroscopy to characterize the growth dynamics of biofilm formation in *Pseudomonas aeruginosa*. *Sci. Rep.* **7**, 5223 (2017).